

CrossDiff: Diffusion Probabilistic Model With Cross-conditional Encoder-Decoder for Crack Segmentation

Xianglong Shi¹, Yunhan Jiang¹, Xiaoheng Jiang^{1*}, Mingling Xu¹, Yang Liu²

¹Zhengzhou University

²King's College London

csxlshi@163.com, yhjiang@stu.zzu.edu.cn, {jiangxiaoheng, iexumingliang}@zzu.edu.cn, yang.9.liu@kcl.ac.uk

Abstract

Crack Segmentation in industrial concrete surfaces is a challenging task because cracks usually exhibit intricate morphology with slender appearances. Traditional segmentation methods often struggle to accurately locate such cracks, leading to inefficiencies in maintenance and repair processes. In this paper, we propose a novel diffusion-based model with a cross-conditional encoder-decoder, named CrossDiff, which is the first to introduce the diffusion probabilistic model for the crack segmentation task. Specifically, CrossDiff integrates a cross-encoder and a cross-decoder into the diffusion model to constitute a cross-shaped diffusion model structure. The cross-encoder enhances the ability to retain crack details and the cross-decoder helps extract the semantic features of cracks. As a result, CrossDiff can better handle slender cracks. Extensive experiments were conducted on five challenging crack datasets including CFD, CrackTree200, DeepCrack, GAPs384, and Rissbilder. The results demonstrate that the proposed CrossDiff model achieves impressive performance, outperforming other state-of-the-art methods by 8.0% in terms of both Dice score and IoU. The code will be open-source soon.

Introduction

Industrial concrete surfaces, such as roads and pavements (Koch et al. 2015; König et al. 2022; Kheradmandi and Mehranfar 2022; Du et al. 2023), are susceptible to the formation of cracks over time due to various factors including traffic load (Nguyen et al. 2023), temperature fluctuations (Kheradmandi and Mehranfar 2022), and environmental conditions (Munawar et al. 2021). These cracks not only compromise the structural integrity of the surfaces but also pose safety hazards to vehicles and pedestrians. Effective maintenance and repair strategies necessitate accurate segmentation of these cracks to identify their extent and severity (Hüthwohl and Brilakis 2018; Choi and Cha 2019; Panella, Lipani, and Boehm 2022). However, segmentation of cracks remains a challenging task due to their intricate morphology and the presence of noise and artifacts in the concrete surface images.

In addition to their complex morphology, as shown in Figure 1, long-narrow cracks often manifest low contrast or irregular intensity profiles, further complicating their segmen-

tation. Variations in illumination, imaging conditions, or material properties can obscure these cracks, making their detection and delineation challenging (Khan et al. 2023). The presence of noise and artifacts in real-world imaging scenarios further compounds the segmentation task by introducing spurious features that may interfere with accurate crack identification.

Deep learning techniques, particularly Convolutional Neural Networks (CNNs) (Zhou et al. 2018; He et al. 2017; Chen et al. 2018) and attention mechanisms (as seen in Transformer models (Cheng et al. 2022; Xie et al. 2021; Kirillov et al. 2023)), have demonstrated remarkable success in various image processing tasks, especially in segmentation (Xie et al. 2021; Cheng, Schwing, and Kirillov 2021; Cheng et al. 2022). However, applying these techniques to the segmentation of slender cracks in concrete surfaces still presents unique challenges. For instance, CNN-based methods (Choi and Cha 2019; Pang et al. 2022; Du et al. 2023) are inherently limited in capturing fine-grained details, especially in regions with subtle variations in texture and color. Additionally, slender cracks often exhibit irregular shapes and low contrast (Tabernik, Šuc, and Skočaj 2023), making them difficult to distinguish from background clutter and noise. While attention mechanisms, such as those employed in Transformer models (Zhou, Zhang, and Gong 2023; Ding et al. 2023; Guo et al. 2023), can help prioritize relevant information (Vaswani et al. 2017), they still struggle to effectively capture the spatial relationships between pixels in long and narrow structures.

In this study, we introduce CrossDiff, a novel Diffusion Probabilistic Model (DPM) (Ho, Jain, and Abbeel 2020; Nichol and Dhariwal 2021) architecture with cross-conditional encoding and decoding, for slender crack segmentation. By integrating cross-conditional information exchange and probabilistic modeling, CrossDiff aims to overcome the inherent challenges associated with detecting and delineating slender cracks across various imaging modalities. Our approach leverages the strengths of deep learning to learn informative representations from data while incorporating probabilistic modeling to capture uncertainty and enhance segmentation accuracy. Through comprehensive experimental evaluations on diverse datasets, including CFD (Shi et al. 2016), CrackTree-200 (Zou et al. 2012), DeepCrack (Liu et al. 2019), GAPs384 (Eisenbach et al.

*Corresponding Author

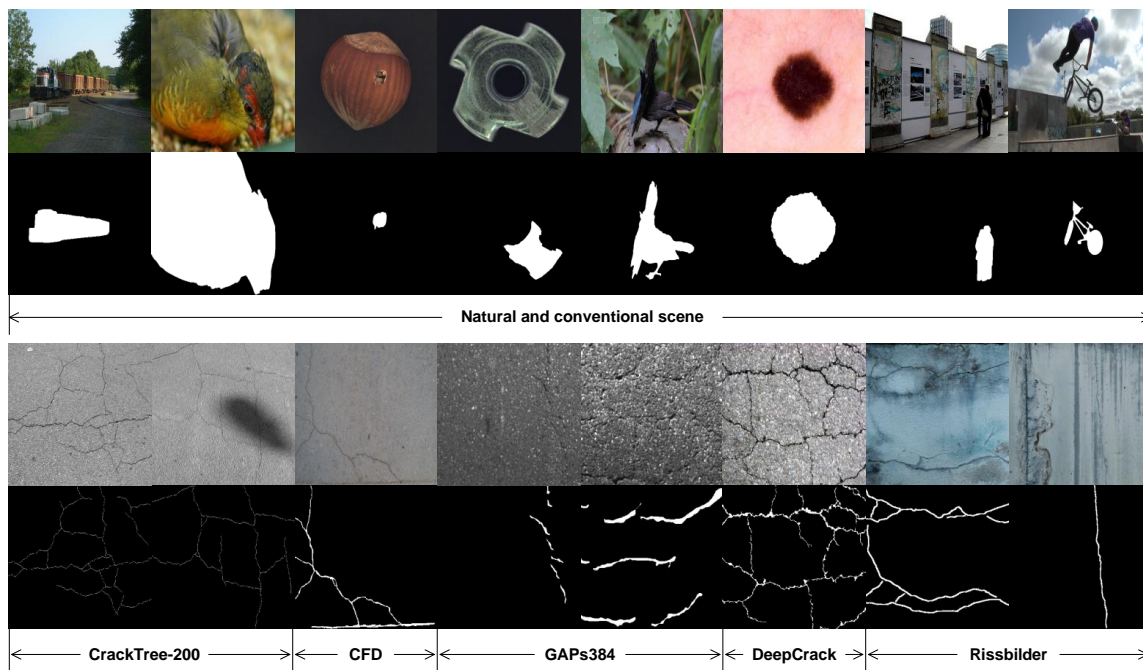


Figure 1: Comparison between natural and conventional scene images with industrial crack images. The top row showcases images from mainstream semantic segmentation datasets, including Pascal VOC (Everingham et al. 2015), MVTecAD (Bergmann et al. 2019), SegTrack-v2 (Li et al. 2013) and ISIC (Gutman et al. 2016), with corresponding ground truth images in the second row. The third row displays samples from CFD (Shi et al. 2016), CrackTree-200 (Zou et al. 2012), DeepCrack (Liu et al. 2019), GAPs384 (Eisenbach et al. 2017), and Rissbilder (Pak and Kim 2021) with their ground truth images below.

2017), and Rissbilder (Pak and Kim 2021), we demonstrate the efficacy and generalization capabilities of CrossDiff in addressing the challenging task of slender crack segmentation.

In summary, our paper makes the following contributions:

- The first to introduce Diffusion Probabilistic Model-based framework for crack detection and prove its efficiency toward slender crack segmentation, as evidenced by the formulaic validation and experimental data.
- We propose a novel Cross-Conditional DPM architecture, CrossDiff, which takes advantage of a Cross Encoder and a Cross Decoder to jointly enhance the ability to extract crack features.
- Our proposed model demonstrates superior segmentation performance compared to other state-of-the-art methods on all five challenging crack datasets, achieving notable improvements in terms of Intersection over Union (IoU) and Dice score.

Related Work

Discriminant Segmentation

After the introduction of pixel-level asphalt crack detection utilizing CNN models by Zhang (Zhang et al. 2017), several more precise approaches have emerged for analyzing pavement damage employing deep neural networks (Zou et al. 2018; Yang et al. 2019; Fei et al. 2019). For instance, Liu (Maeda et al. 2018) introduced a network for

pyramid features aggregation along with a post-processing scheme employing Conditional Random Fields (CRFs) to enhance crack segmentation. Zou (Zou et al. 2018) proposed a multi-stage fusion approach built upon the SegNet encoder-decoder architecture to refine crack segmentation. Yang (Yang et al. 2019) presented a hierarchical boosting network combined with a feature pyramid for pavement crack detection, effectively integrating contextual information into low-level features in a feature-pyramid manner. Fei (Fei et al. 2019) introduced the CrackNet-V model, which incorporates stacked 3×3 convolutional layers and a 15×15 convolution kernel to achieve deep abstraction and high performance in crack segmentation.

Then CrackFormer (Liu et al. 2021) employs a Transformer network architecture featuring multi-head attention mechanisms, positional encoding, and an encoder-decoder framework to effectively capture long-range dependencies and spatial relationships within images, enabling precise fine-grained crack detection across various surfaces and conditions. Tabernik (Tabernik, Šuc, and Skočaj 2023) proposes a novel approach that combines per-pixel segmentation and per-image classification. Their model leverages an encoder-decoder architecture to achieve accurate segmentation results, while also maintaining low computational costs for real-time applications. Despite the promising results achieved by these segmentation-based crack detection methods, they often fall short in attaining satisfactory pixel-

level segmentation precision, resulting in blurred and coarse segmentation outcomes.

Generative Segmentation

Generative segmentation, a burgeoning field in image analysis, has witnessed remarkable progress in recent years. Various approaches, including classical methods such as Markov Random Fields (MRFs) and Conditional Random Fields (CRFs), which model pixel dependencies, and deep generative models like Generative Adversarial Networks (GANs) and Variational Autoencoders (VAEs), have been explored for generative segmentation tasks. GANs produce realistic images through adversarial training, while VAEs learn latent representations and reconstruct images. Recently, the Diffusion Probabilistic Model (DPM) has emerged as a prominent topic in computer vision, attracting significant attention within the research community. Its applications in image generation, such as DALLE3 (Betker et al. 2023), Imagen (Saharia et al. 2022), and Stable Diffusion (Rombach et al. 2022), have showcased remarkable generation capabilities, sparking extensive discussions. Moreover, recent studies have demonstrated its utility in image segmentation tasks, such as DMOISE (Wolleb et al. 2022), SegDiff (Amit et al. 2021), MedSegDiff (Wu et al. 2024) and MedSeg-Diff-v2 (Wu et al. 2024).

Method

In this section, we present the methodology employed in our proposed approach, CrossDiff, for the segmentation of slender cracks in industrial concrete surfaces. We present the foundational component of our method, the Diffusion Probabilistic Model (DPM), which serves as the backbone for capturing spatial dependencies and promoting coherence in the segmentation results. Following this, we present the Cross-conditional network, a novel architecture designed to enhance feature representation and capture fine-grained details, particularly in regions with subtle variations. In final, we present the training process and its impact on the overall architecture of our model, elucidating how these components synergistically contribute to achieving superior performance in crack segmentation tasks.

Towards Generative Slender Segmentation

Our model architecture draws inspiration from the diffusion model discussed in (Ho, Jain, and Abbeel 2020) and (Nichol and Dhariwal 2021), which constitutes a generative framework comprising a forward diffusion stage and a reverse diffusion stage. In the forward process, Gaussian noise is gradually incorporated into the segmentation label x_0 over a series of iterations T . Conversely, the reverse process employs a neural network to reconstruct the original data by undoing the noise addition, formulated as:

$$p(x_{0:T-1}|x_T) = \prod_{t=1}^T p(x_{t-1}|x_t), \quad (1)$$

where $x_{0:T-1}$ represents the sequence of latent variables, and x_T is the final noisy image. To ensure symmetry with

the forward process, the reverse diffusion recovers the noise image step by step, ultimately yielding a clear segmentation.

In our implementation, we adopt a UNet architecture as the neural network for learning, as depicted in Figure 2 (Diffusion Encoder and Diffusion Decoder). To facilitate segmentation, we condition the step estimation function ϵ by incorporating raw image priors:

$$\epsilon(x_t, I, t) = D((E_{I_t} + E_{x_t}, t), t), \quad (2)$$

where E_{I_t} denotes the conditional feature embedding derived from the raw image by Cross Encoder, while E_{x_t} represents the segmentation map feature embedding at the current step. These embeddings are combined and processed by a UNet decoder D for reconstruction, with the step-index t integrated into the process via a shared learned look-up table, following (Ho, Jain, and Abbeel 2020).

Diffusion segmentation typically relies on the construction of a graph or network, where nodes represent pixels and edges represent connections between pixels. The weights of connections are usually determined based on the similarity between pixels. Let W_{ij} represent the weight of the connection between nodes i and j . For slender objects, we can assume that pixels within the object have high similarity with each other, as they may share similar color, texture, or shape features. We start with an image I containing a particularly slender object O and background B . Our goal is to segment the object O from the background B . Therefore, for pixels i and j within the object O , the connection weight W_{ij} might be relatively large. Conversely, connections between the object O and the background B may have smaller weights.

Diffusion segmentation involves an information propagation process, where pixel labels (indicating whether they belong to object O or background B) affect the labels of their neighboring pixels. This process can be represented as:

$$L_i^{(t+1)} = \sum_{j \in N(i)} W_{ij} \cdot L_j^{(t)}, \quad (3)$$

where $L_i^{(t)}$ represents the label of pixel i at iteration t , and $N(i)$ denotes the set of neighboring pixels of pixel i . Since pixels within the slender object have high similarity, with larger connection weights, they are more likely to influence each other during the information propagation process, leading to consistent labels within the object. On the other hand, for the background B , where connection weights are smaller, the influence of information propagation may be comparatively weaker.

Thus, through the information propagation process, diffusion segmentation can more easily and stably segment the slender object from the background. This is why diffusion segmentation performs better when dealing with particularly slender objects, leveraging the similarity between pixels during the information propagation process to form consistent regions within the object.

Cross-Conditional Encoder-Decoder

Cross Encoder The Cross Encoder, as shown in Figure 2, inspired by the Vision Transformer (ViT) (Dosovitskiy et al.

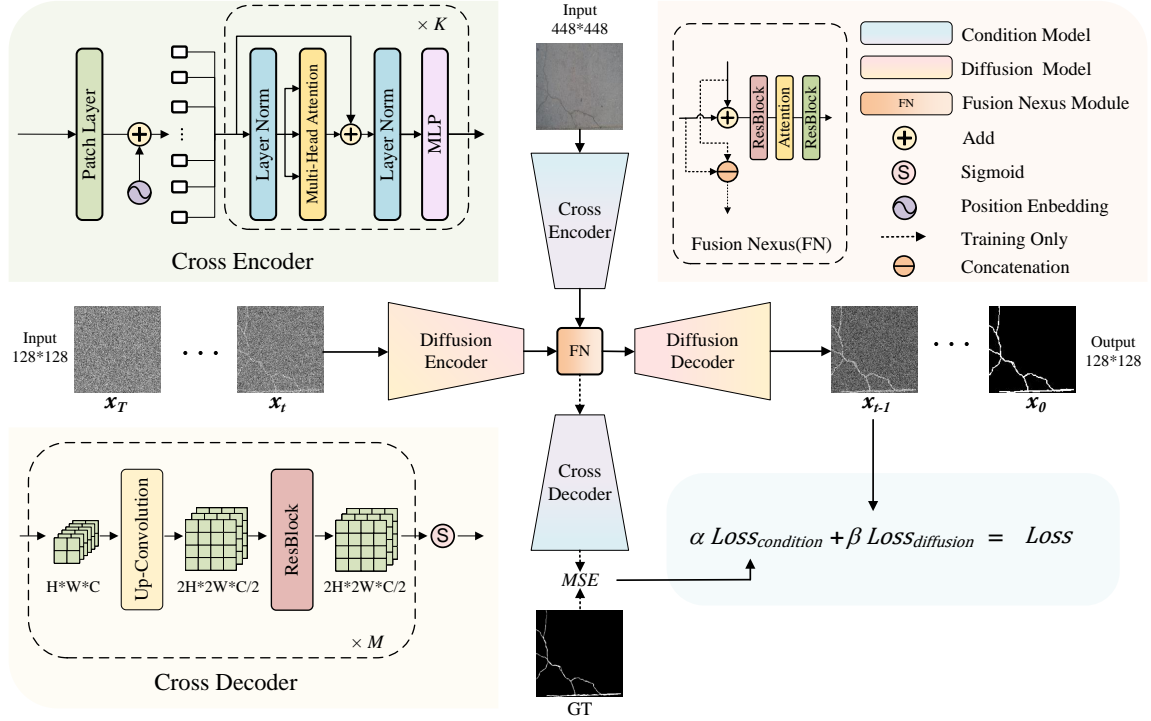


Figure 2: An illustration of CrossDiff. CrossDiff consists of Diffusion backbone and cross-conditional encoder-decoder, including Cross Encoder, Fusion Nexus, and Cross Decoder, which jointly constitute the cross-shaped diffusion model structure.

2020; Kirillov et al. 2023) backbone, consists of patch embedding, positional encoding, Transformer blocks, and a neck module. Patch embedding divides the input image into patches and projects them into a lower-dimensional space. Absolute positional embeddings are added to provide spatial information. Transformer blocks, comprising self-attention and MLP layers, capture global and local dependencies. Finally, the neck module refines the feature representations. The features extracted by this architecture effectively condition the step estimation function in diffusion probabilistic models, enabling precise segmentation of slender cracks in industrial concrete surfaces.

Cross Decoder The Decoder module (Figure 2), is pivotal in reconstructing segmented images from the conditioned features provided by the Conditional Encoder and Diffusion Encoder. It consists of a series of transposed convolutional layers, interleaved with residual blocks, to ensure efficient feature extraction and high-fidelity image reconstruction. Each ResidualBlock within the decoder comprises two transposed convolutional layers, followed by rectified linear unit (ReLU) activation functions and residual connections, facilitating effective learning of residual mappings. The decoder architecture encompasses six transposed convolutional layers, progressively increasing the spatial resolution by a factor of two through each layer, effectively capturing fine-grained details in the reconstruction process. After each transposed convolutional layer, a corresponding ResidualBlock is employed to refine the reconstructed features

further. The final layer of the decoder comprises a transposed convolutional operation followed by a sigmoid activation function, yielding the ultimate segmentation masks. This comprehensive architecture enables the model to decode conditioned features accurately into a segmentation map.

Fusion Nexus Module The middle layer acts as a pivotal bridge between the conditioned Decoder output and the Diffusion Encoder backbone, leveraging the current diffusion step information to intricately balance and fuse features from both sources. This layer consists of residual and attention blocks which dynamically adjust the importance of features according to the diffusion step to ensure adaptive information fusion. The Residual Blocks incorporate time embedding to capture temporal dynamics, while the Attention Block enables context-aware feature adjustment. Through residual connections and attentive processing, the middle layer refines the fused features, optimizing their utilization for segmentation tasks.

Optimization Objectives

To optimize the diffusion encoder and cross encoder, the training loss is computed based on a modified version of Equation in (Ho, Jain, and Abbeel 2020), represented as follows:

$$Loss = \alpha E_{x_0, \epsilon, x_e, t} \left[\|\epsilon - \epsilon_\theta(\sqrt{\alpha_t}x_0 + \sqrt{1 - \alpha_t}x_e, I_i, t)\|_2^2 \right] + \beta (x_{d,t} - x_0)^2. \quad (4)$$

during training, where x_0 represents the segmentation of the input image I_i and $x_{d,t}$ represents the segmentation output

from cross decoder in each iteration, so the loss is computed by setting $x_0 = S$, where S denotes the ground truth segmentation mask. In each iteration, a random pair of raw image I_i and its corresponding segmentation label S_i are sampled for training. The iteration number is sampled from a uniform distribution, and ϵ is sampled from a Gaussian distribution. Furthermore, the design of loss function allows the loss of Cross Decoder to impact both Diffusion Encoder and Cross Encoder. Enhancing the feature extraction capabilities of Diffusion Encoder for x_0 in each step is effective for the final prediction.

Experiments

In this section, we present our experimental evaluation of the proposed method for the surface crack segmentation task. We compare our method with several related state-of-the-art approaches with publicly available code.

Dataset

To validate the effectiveness of our model, we train and evaluate our network on one of the largest datasets proposed by Li (Li et al. 2021) which they compiled from previously published datasets CFD (Shi et al. 2016), CRACK500 (Dorafshan, Thomas, and Maguire 2018), CrackTree200 (Zou et al. 2012), DeepCrack (Liu et al. 2019), GAPs384 (Eisenbach et al. 2017), Rissbilder (Pak and Kim 2021), Non-crack (Dorafshan, Thomas, and Maguire 2018), containing crack of road pavements, asphalt and concrete structures and walls. Datasets totally contain 7169 with manually annotated labels in a resolution of 448×448 pixels. It includes crack images from different environments, with varying sizes, shapes, shooting distances, and covering common crack features to the greatest extent possible.

Evaluation Metrics

The performance of our model for segmentation is assessed using two commonly employed evaluation metrics: Intersection over Union (IoU) and Dice coefficient. IoU measures the degree of overlap between the predicted segmentation mask and the ground truth mask. It is calculated as the ratio of the intersection area between the predicted and ground truth masks to their union. A higher IoU score indicates better alignment between the predicted and ground truth anomalies. The Dice coefficient, also known as the F1 score, quantifies the similarity between the predicted and ground truth segmentation masks. It is computed as twice the intersection area divided by the sum of areas of the predicted and ground truth masks. Like IoU, a higher Dice coefficient signifies better segmentation accuracy.

Implementation Details

The proposed architecture is implemented in PyTorch framework and trained/tested on a 4090 GPU with 24GB of memory. All images are uniformly resized to the dimension of 128×128 pixels for Diffusion Encoder and 448×448 pixels for Cross Encoder. The networks are trained in an end-to-end manner using AdamW (Loshchilov and Hutter 2017)

optimizer. CrossDiff is trained with 12 batch size. The learning rate is initially set to $1e-4$. The Cross Decoder is only utilized during training. All models are set 5 times of ensemble in the inference. We use STAPLE (Warfield, Zou, and Wells 2004) algorithm to fuse the different samples.

Main Results

To verify the slender crack image segmentation performance, we compare CrossDiff with SOTA segmentation methods on multi-crack segmentation datasets. The quantitative results of Dice score and IoU are shown in Table 1 and Figure 3 respectively. In Table 1, we compare the segmentation methods which are widely used and well-recognized in the community, including the typical image segmentation method DeepLabv3+ (Chen et al. 2018)(Chen 2018), and crack segmentation method the CNN-based method SCCDNet-D32 (Li et al. 2021)(Li 2021), DeepCrack (Liu et al. 2019)(Liu 2019), SegDecNet++ (Tabernik, Šuc, and Skočaj 2023)(Tabernik 2023) and the transformer-based method CrackFormer (Liu et al. 2021)(Liu 2021)), in which SegDecNet++ is SOTA method before.

From Table 1, it is evident that CrossDiff outperforms all other methods across five different tasks, underscoring its exceptional generalization prowess across diverse crack segmentation tasks and image modalities. Traditional methods exhibit subpar performance on the CrackTree200 dataset due to the unique characteristics of crack size. In comparison to SegDecNet++, CrossDiff demonstrates an average improvement of 8 percentage points in terms of IoU, especially in CFD and CrackTree200 which feature more slender cracks compared to the other three datasets. Although the IoU achieved by CrossDiff for the CrackTree200 dataset is only 38.34%, Figure 3 illustrates that the predictions are capable of roughly localizing the cracks. Furthermore, CrossDiff exhibits superior performance stability at threshold levels compared to the second best method SegDecNet++, as demonstrated in Table 2.

Ablation Studies

We do a comprehensive ablation study to verify the effectiveness of the proposed Cross Encoder and Cross Decoder. The results are shown in Table 3, where 448 and 1024 donate the input size of Cross Encoder and the parameter complexity of its ViT backbone (K in Figure 2), while layer12 and layer34 donate the number of layers (M in Figure 2) in CrossDecoder. We evaluate the performance by average Dice score(%) and IoU(%) on all five tasks. Cross Encoder and Cross Decoder improve 1.36% and 1.35% in average IoU. However, we observe that as the complexity of the Cross Encoder and Cross Decoder increases, it is difficult for the model to converge.

Conclusion

In this paper, we introduce a Diffusion Probabilistic Model (DPM)-based approach and demonstrate its effectiveness in segmenting slender cracks. Furthermore, we present a novel cross-conditional DPM architecture, named CrossDiff comprising Cross Encoder and Cross Decoder. Through compar-

Method	CFD		CrackTree200		DeepCrack		GAPs384		Rissbilder	
	Dice	IoU	Dice	IoU	Dice	IoU	Dice	IoU	Dice	IoU
DeepLabv3+	73.84	59.28	01.70	00.86	82.80	72.04	53.82	38.69	76.11	64.91
SCCDNet-D32	65.59	49.47	03.88	02.04	78.08	65.47	52.86	37.81	71.78	56.86
DeepCrack	67.84	51.94	05.10	02.67	76.57	63.61	48.94	34.88	70.98	56.13
CrackFormer	71.52	56.16	35.46	21.65	79.61	67.89	55.18	40.03	72.22	58.06
SegDecNet++	77.80	64.14	33.02	20.12	81.17	69.78	54.36	39.05	80.40	67.95
CrossDiff	91.34	85.54	55.10	38.34	85.30	76.07	55.41	41.11	85.55	75.98

Table 1: The comparison of CrossDiff with SOTA segmentation methods over the five datasets evaluated by Dice Score and IoU. The best results are highlighted in bold.

Threshold (θ)	0.1		0.3		0.5		0.7		0.9		0.95	
	Dice	IoU	Dice	IoU	Dice	IoU	Dice	IoU	Dice	IoU	Dice	IoU
SegDecNet++	65.26	49.80	68.94	53.73	71.34	56.52	73.75	59.30	77.43	63.61	75.67	62.87
CrossDiff	81.17	70.77	81.72	71.61	81.72	71.61	81.72	71.61	81.31	71.01	76.64	64.20

Table 2: The comparison of CrossDiff with the second best method on different thresholds over the five datasets. Average is the average Dice score and IoU of five datasets, weighted by sample numbers.

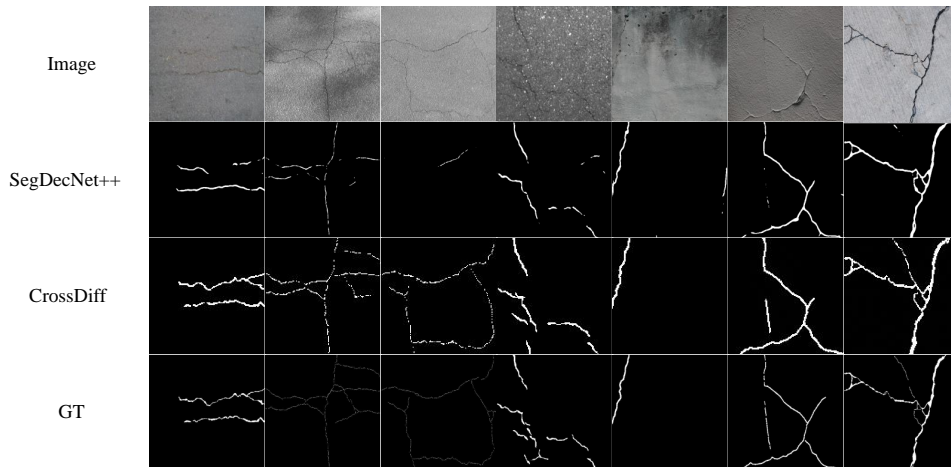


Figure 3: The sequence of images, progressing from top to bottom, includes the input image, SegDecNet++ (Tabernik, Šuc, and Skočaj 2023), CrossDiff, and ground truth mask (GT). It is apparent from the visual comparison that our model surpasses SegDecNet++ (Tabernik, Šuc, and Skočaj 2023) in terms of the accuracy of cracks localization.

Cross Encoder		Cross Decoder		Average	
448	1024	12 layers	34 layers	Dice	IoU
×	×	×	×	79.61	68.90
✓	×	×	×	80.77	70.26
✓	×	✓	×	81.72	71.61
×	✓	×	✓	79.85	68.84
✓	×	×	✓	79.74	68.74

Table 3: An ablation study on Cross Encoder and Cross Decoder. Average is the average Dice score and IoU of five datasets, weighted by sample numbers.

ative experiments conducted on five crack datasets, Cross-Diff shows superior performance in Dice score and IoU compared to previous state-of-the-art approaches. As the first proposed cross-conditional architecture applying DPM to crack segmentation, we believe that our proposed cross-design will serve as an essential architecture for future research.

References

- Amit, T.; Shaharabany, T.; Nachmani, E.; and Wolf, L. 2021. Segdiff: Image segmentation with diffusion probabilistic models. *arXiv preprint arXiv:2112.00390*.
- Bergmann, P.; Fauser, M.; Sattlegger, D.; and Steger, C. 2019. MVTec AD—A comprehensive real-world dataset for unsupervised anomaly detection. In *Proceedings of the IEEE/CVF conference on computer vision and pattern recognition*, 9592–9600.
- Betker, J.; Goh, G.; Jing, L.; Brooks, T.; Wang, J.; Li, L.; Ouyang, L.; Zhuang, J.; Lee, J.; Guo, Y.; et al. 2023. Improving image generation with better captions. *Computer Science*. <https://cdn.openai.com/papers/dall-e-3.pdf>, 2(3): 8.
- Chen, L.-C.; Zhu, Y.; Papandreou, G.; Schroff, F.; and Adam, H. 2018. Encoder-decoder with atrous separable convolution for semantic image segmentation. In *Proceedings of the European conference on computer vision (ECCV)*, 801–818.
- Cheng, B.; Misra, I.; Schwing, A. G.; Kirillov, A.; and Girdhar, R. 2022. Masked-attention mask transformer for universal image segmentation. In *Proceedings of the IEEE/CVF conference on computer vision and pattern recognition*, 1290–1299.
- Cheng, B.; Schwing, A.; and Kirillov, A. 2021. Per-pixel classification is not all you need for semantic segmentation. *Advances in neural information processing systems*, 34: 17864–17875.
- Choi, W.; and Cha, Y.-J. 2019. SDDNet: Real-time crack segmentation. *IEEE Transactions on Industrial Electronics*, 67(9): 8016–8025.
- Ding, W.; Yang, H.; Yu, K.; and Shu, J. 2023. Crack detection and quantification for concrete structures using UAV and transformer. *Automation in Construction*, 152: 104929.
- Dorafshan, S.; Thomas, R. J.; and Maguire, M. 2018. SD-NET2018: An annotated image dataset for non-contact concrete crack detection using deep convolutional neural networks. *Data in brief*, 21: 1664–1668.
- Dosovitskiy, A.; Beyer, L.; Kolesnikov, A.; Weissenborn, D.; Zhai, X.; Unterthiner, T.; Dehghani, M.; Minderer, M.; Heigold, G.; Gelly, S.; et al. 2020. An image is worth 16x16 words: Transformers for image recognition at scale. *arXiv preprint arXiv:2010.11929*.
- Du, Y.; Zhong, S.; Fang, H.; Wang, N.; Liu, C.; Wu, D.; Sun, Y.; and Xiang, M. 2023. Modeling automatic pavement crack object detection and pixel-level segmentation. *Automation in Construction*, 150: 104840.
- Eisenbach, M.; Stricker, R.; Seichter, D.; Amende, K.; Debes, K.; Sesselmann, M.; Ebersbach, D.; Stoeckert, U.; and Gross, H.-M. 2017. How to get pavement distress detection ready for deep learning? A systematic approach. In *2017 international joint conference on neural networks (IJCNN)*, 2039–2047. IEEE.
- Everingham, M.; Eslami, S. A.; Van Gool, L.; Williams, C. K.; Winn, J.; and Zisserman, A. 2015. The pascal visual object classes challenge: A retrospective. *International journal of computer vision*, 111: 98–136.
- Fei, Y.; Wang, K. C.; Zhang, A.; Chen, C.; Li, J. Q.; Liu, Y.; Yang, G.; and Li, B. 2019. Pixel-level cracking detection on 3D asphalt pavement images through deep-learning-based CrackNet-V. *IEEE Transactions on Intelligent Transportation Systems*, 21(1): 273–284.
- Guo, F.; Qian, Y.; Liu, J.; and Yu, H. 2023. Pavement crack detection based on transformer network. *Automation in Construction*, 145: 104646.
- Gutman, D.; Codella, N. C.; Celebi, E.; Helba, B.; Marchetti, M.; Mishra, N.; and Halpern, A. 2016. Skin lesion analysis toward melanoma detection: A challenge at the international symposium on biomedical imaging (ISBI) 2016, hosted by the international skin imaging collaboration (ISIC). *arXiv preprint arXiv:1605.01397*.
- He, K.; Gkioxari, G.; Dollár, P.; and Girshick, R. 2017. Mask r-cnn. In *Proceedings of the IEEE international conference on computer vision*, 2961–2969.
- Ho, J.; Jain, A.; and Abbeel, P. 2020. Denoising diffusion probabilistic models. *Advances in neural information processing systems*, 33: 6840–6851.
- Hüthwohl, P.; and Brilakis, I. 2018. Detecting healthy concrete surfaces. *Advanced Engineering Informatics*, 37: 150–162.
- Khan, M. A.-M.; Kee, S.-H.; Pathan, A.-S. K.; and Nahid, A.-A. 2023. Image Processing Techniques for Concrete Crack Detection: A Scientometrics Literature Review. *Remote Sensing*, 15(9): 2400.
- Kheradmandi, N.; and Mehranfar, V. 2022. A critical review and comparative study on image segmentation-based techniques for pavement crack detection. *Construction and Building Materials*, 321: 126162.
- Kirillov, A.; Mintun, E.; Ravi, N.; Mao, H.; Rolland, C.; Gustafson, L.; Xiao, T.; Whitehead, S.; Berg, A. C.; Lo, W.-Y.; et al. 2023. Segment anything. In *Proceedings of the IEEE/CVF International Conference on Computer Vision*, 4015–4026.
- Koch, C.; Georgieva, K.; Kasireddy, V.; Akinci, B.; and Fieguth, P. 2015. A review on computer vision based defect detection and condition assessment of concrete and asphalt civil infrastructure. *Advanced engineering informatics*, 29(2): 196–210.
- König, J.; Jenkins, M.; Mannion, M.; Barrie, P.; and Morrison, G. 2022. What’s Cracking? A Review and Analysis of Deep Learning Methods for Structural Crack Segmentation, Detection and Quantification. *arXiv preprint arXiv:2202.03714*.

- Li, F.; Kim, T.; Humayun, A.; Tsai, D.; and Rehg, J. M. 2013. Video segmentation by tracking many figure-ground segments. In *Proceedings of the IEEE international conference on computer vision*, 2192–2199.
- Li, H.; Yue, Z.; Liu, J.; Wang, Y.; Cai, H.; Cui, K.; and Chen, X. 2021. Sccdnet: A pixel-level crack segmentation network. *Applied Sciences*, 11(11): 5074.
- Liu, H.; Miao, X.; Mertz, C.; Xu, C.; and Kong, H. 2021. CrackFormer: Transformer Network for Fine-Grained Crack Detection. In *2021 IEEE/CVF International Conference on Computer Vision (ICCV)*, 3763–3772.
- Liu, Y.; Yao, J.; Lu, X.; Xie, R.; and Li, L. 2019. DeepCrack: A deep hierarchical feature learning architecture for crack segmentation. *Neurocomputing*, 338: 139–153.
- Loshchilov, I.; and Hutter, F. 2017. Decoupled weight decay regularization. *arXiv preprint arXiv:1711.05101*.
- Maeda, H.; Sekimoto, Y.; Seto, T.; Kashiyama, T.; and Omata, H. 2018. Road damage detection and classification using deep neural networks with smartphone images. *Computer-Aided Civil and Infrastructure Engineering*, 33(12): 1127–1141.
- Munawar, H. S.; Hammad, A. W.; Haddad, A.; Soares, C. A. P.; and Waller, S. T. 2021. Image-based crack detection methods: A review. *Infrastructures*, 6(8): 115.
- Nguyen, S. D.; Tran, T. S.; Tran, V. P.; Lee, H. J.; Piran, M. J.; and Le, V. P. 2023. Deep learning-based crack detection: A survey. *International Journal of Pavement Research and Technology*, 16(4): 943–967.
- Nichol, A. Q.; and Dhariwal, P. 2021. Improved denoising diffusion probabilistic models. In *International conference on machine learning*, 8162–8171. PMLR.
- Pak, M.; and Kim, S. 2021. Crack detection using fully convolutional network in wall-climbing robot. In *Advances in Computer Science and Ubiquitous Computing: CSA-CUTE 2019*, 267–272. Springer.
- Panella, F.; Lipani, A.; and Boehm, J. 2022. Semantic segmentation of cracks: Data challenges and architecture. *Automation in Construction*, 135: 104110.
- Pang, J.; Zhang, H.; Zhao, H.; and Li, L. 2022. DcsNet: a real-time deep network for crack segmentation. *Signal, Image and Video Processing*, 1–9.
- Rombach, R.; Blattmann, A.; Lorenz, D.; Esser, P.; and Ommer, B. 2022. High-resolution image synthesis with latent diffusion models. In *Proceedings of the IEEE/CVF conference on computer vision and pattern recognition*, 10684–10695.
- Saharia, C.; Chan, W.; Saxena, S.; Li, L.; Whang, J.; Denton, E. L.; Ghasemipour, K.; Gontijo Lopes, R.; Karagol Ayan, B.; Salimans, T.; et al. 2022. Photorealistic text-to-image diffusion models with deep language understanding. *Advances in neural information processing systems*, 35: 36479–36494.
- Shi, Y.; Cui, L.; Qi, Z.; Meng, F.; and Chen, Z. 2016. Automatic road crack detection using random structured forests. *IEEE Transactions on Intelligent Transportation Systems*, 17(12): 3434–3445.
- Tabernik, D.; Šuc, M.; and Skočaj, D. 2023. Automated detection and segmentation of cracks in concrete surfaces using jointed segmentation and classification deep neural network. *Construction and Building Materials*, 408: 133582.
- Vaswani, A.; Shazeer, N.; Parmar, N.; Uszkoreit, J.; Jones, L.; Gomez, A. N.; Kaiser, Ł.; and Polosukhin, I. 2017. Attention is all you need. *Advances in neural information processing systems*, 30.
- Warfield, S. K.; Zou, K. H.; and Wells, W. M. 2004. Simultaneous truth and performance level estimation (STAPLE): an algorithm for the validation of image segmentation. *IEEE transactions on medical imaging*, 23(7): 903–921.
- Wolleb, J.; Sandkühler, R.; Bieder, F.; Valmaggia, P.; and Cattin, P. C. 2022. Diffusion models for implicit image segmentation ensembles. In *International Conference on Medical Imaging with Deep Learning*, 1336–1348. PMLR.
- Wu, J.; Fu, R.; Fang, H.; Zhang, Y.; Yang, Y.; Xiong, H.; Liu, H.; and Xu, Y. 2024. Medsegdiff: Medical image segmentation with diffusion probabilistic model. In *Medical Imaging with Deep Learning*, 1623–1639. PMLR.
- Xie, E.; Wang, W.; Yu, Z.; Anandkumar, A.; Alvarez, J. M.; and Luo, P. 2021. SegFormer: Simple and efficient design for semantic segmentation with transformers. *Advances in neural information processing systems*, 34: 12077–12090.
- Yang, F.; Zhang, L.; Yu, S.; Prokhorov, D.; Mei, X.; and Ling, H. 2019. Feature pyramid and hierarchical boosting network for pavement crack detection. *IEEE Transactions on Intelligent Transportation Systems*, 21(4): 1525–1535.
- Zhang, A.; Wang, K. C.; Li, B.; Yang, E.; Dai, X.; Peng, Y.; Fei, Y.; Liu, Y.; Li, J. Q.; and Chen, C. 2017. Automated pixel-level pavement crack detection on 3D asphalt surfaces using a deep-learning network. *Computer-Aided Civil and Infrastructure Engineering*, 32(10): 805–819.
- Zhou, Z.; Rahman Siddiquee, M. M.; Tajbakhsh, N.; and Liang, J. 2018. Unet++: A nested u-net architecture for medical image segmentation. In *Deep Learning in Medical Image Analysis and Multimodal Learning for Clinical Decision Support: 4th International Workshop, DLMIA 2018, and 8th International Workshop, ML-CDS 2018, Held in Conjunction with MICCAI 2018, Granada, Spain, September 20, 2018, Proceedings 4*, 3–11. Springer.
- Zhou, Z.; Zhang, J.; and Gong, C. 2023. Hybrid semantic segmentation for tunnel lining cracks based on Swin Transformer and convolutional neural network. *Computer-Aided Civil and Infrastructure Engineering*, 38(17): 2491–2510.
- Zou, Q.; Cao, Y.; Li, Q.; Mao, Q.; and Wang, S. 2012. CrackTree: Automatic crack detection from pavement images. *Pattern Recognition Letters*, 33(3): 227–238.
- Zou, Q.; Zhang, Z.; Li, Q.; Qi, X.; Wang, Q.; and Wang, S. 2018. Deepcrack: Learning hierarchical convolutional features for crack detection. *IEEE transactions on image processing*, 28(3): 1498–1512.